

ALMA Memo #533 *

Improving Accuracy of Superconducting Microstrip Line Modelling at Millimetre and Sub-Millimetre Waves

Victor Belitsky[†], Christophe Risacher^{†‡}, Miroslav Pantaleev[†], Vessen Vassilev[†]

Abstract— This paper presents a new model to calculate the characteristic impedance and wave propagation constant of a microstrip line made of a superconducting material. Modelling provides the only tool for designing superconducting microstrip - based circuits because no direct measurements of such a line can be made at millimetre and sub-millimetre waves and at cryogenic temperature of 4 K with required high accuracy. In contrast to a conventional microstrip, in the superconducting microstrip line, produced usually by a thin-film technology, the magnetic field penetration depth is comparable with the thicknesses of the dielectric and the superconductors comprising the line. As a result, the electromagnetic wave is propagating not only in the dielectric media but also partly inside the superconducting strip and ground electrodes creating dramatic changes in the line performance that should be carefully accounted for by including the superconductor material properties into the model.

Niobium, as the most commonly exploited superconducting material, was used for the modelling, though the same approach would work for any different BCS superconductor. In order to evaluate the proposed model accuracy, we have made an extensive comparison study of the previously presented models and included 3D numerical electromagnetic simulation. The modelling covers different geometries of the superconducting microstrip line and address material dispersion.

Index Terms—Superconducting microstrip line, characteristic impedance, wave propagation constant, modelling.

I. INTRODUCTION

SUPERCONDUCTOR – insulator - superconductor (SIS) tunnel junction mixers are the dominating technology for millimetre and sub-millimetre wave heterodyne receivers for radio astronomy [1] – [3]. The large intrinsic capacitance of SIS junction makes it difficult to achieve ultimate performance and wide operational frequency band at these extremely high frequencies. A typical approach to solve this problem is to integrate a tuning circuitry on the same substrate; the circuitry resonates out the SIS junction capacitance and can be fabricated during the same processing steps as the SIS junction itself. The microstrip is a natural

choice for that tuning circuitry due to its complete compatibility with the SIS fabrication tri-layer process, low RF loss and flexibility.

The modelling accuracy of a superconducting microstrip line (SML) introduces one of the major challenges in the design of tuning circuitry for SIS mixers. In the thin-film SML, the *magnetic* field penetration depth is comparable with the thicknesses of the dielectric and the superconductors forming the line; this produces radical changes in the line performance. The energy stored in the layers of the superconducting strip and ground electrodes, where H-field penetrates in, becomes comparable with the energy of the electromagnetic wave propagating in the dielectric and thus strongly affects the performance of the SML. Therefore, compared to a conventional microstrip, the modelling of the SML should involve accurate description of the superconducting material properties and its influence on the SML characteristic impedance and the propagation constant.

The purpose of this article is to present a new model for SML and evaluate its accuracy by comparison with previously suggested models [4] – [8] and numerically simulated SML using a 3D electromagnetic simulation package. Direct experimental measurements of a superconducting transmission line at millimetre and sub-millimetre wavelengths cannot provide necessary precision and are extremely difficult at this high frequencies and challenging technically because the object of measurement is in a cryostat at 4 K ambient temperature.

II. SUPERCONDUCTING MICROSTRIP TRANSMISSION LINE

SML has the same geometry as a conventional microstrip transmission line (depicted in Fig. 1) with both strip and ground conductors made of a superconductor material. In this article, we will consider the line strip and ground made of low- T_c BCS superconducting materials [9]. Nb superconductor is used in the model calculations through the whole paper as the most widely exploited material for superconducting thin-film technology.

We are interested in the microstrip lines where the dielectric thickness is *comparable* with the magnetic field penetration depth, London penetration depth, λ_o , as well as with the thicknesses of the strip and ground superconductors forming the line. These particular relations between the strip, ground

* Submitted to ALMA Memo series in 2005.

[†] The authors are with the Group for Advanced Receiver Development, Radio and Space Science Department, Onsala Space Observatory at Chalmers University of Technology, SE 41296, Gothenburg, Sweden

[‡] Christophe Risacher is with APEX/ESO.

and dielectric thicknesses reflect a typical geometry of the superconducting microstrip line produced by a thin-film technology used for, e.g., SIS junction fabrication [10], [11]. In this article, we compare the accuracy of different models for calculations of the line characteristic impedance, propagation constant and its dispersion. Additionally, we present the results of the simulation with High Frequency Structure Simulator, HFSS [12]; we modelled the superconducting material conducting properties via its surface

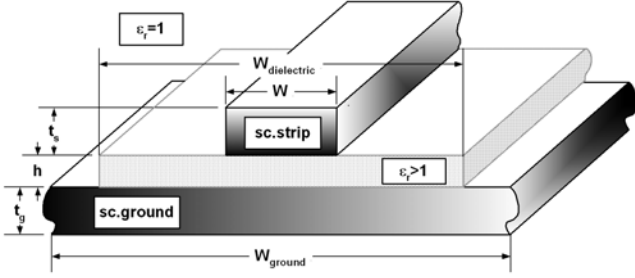


Fig. 1. Schematic view of the superconducting microstrip line. The strip conductor thickness, t_s , ground conductor thickness t_g and the dielectric thickness h considered to be comparable with the static penetration depth of magnetic field, λ_o , while the widths are as following $W_{ground} \gg W_{dielectric} \gg W$.

impedance as proposed in [13].

III. RF CONDUCTIVITY OF A SUPERCONDUCTOR

In contrast with conventional conductors the DC and RF currents in superconducting materials are carried mainly by dual-electron carriers (Cooper pairs) without any conducting loss (super-current). A part of the current associated with loss is carried by quasiparticles (single electrons and holes) generated by thermal excitations and interaction of electromagnetic field and the Cooper pairs. The presence of the energy gap in the electron density of states, $\Delta = \Delta(T)$ ($e\Delta \approx 1.5$ mV for Nb material), limits the ability of the Cooper pairs to carry the RF current at frequencies closer to the gap frequency, $F_g = 2e\Delta/h$, where e is the electron charge, h is the Planck's constant and F_g is the gap frequency. Above F_g the conducting properties of the superconductor become close to that of a conventional conductor.

The magnetic field penetrates into the superconductor within a characteristic depth defined as the static London penetration depth, λ_o , for the DC current. The actual magnetic field penetration depth, λ , has a noticeable frequency dependence for frequencies even well below the gap frequency and, as the frequency approaches the gap frequency of the superconducting material, λ becomes highly frequency dependent [14]–[16]. The microstrip line with the superconducting electrodes becomes material-dispersive and, above the gap frequency, has additionally an increased conducting loss in the strip and ground electrodes due to breaking of Cooper pairs [17], [18].

Mattis – Bardeen theory [19] of the skin anomalous effect describes the behaviour of a superconductor vs. frequency in terms of the complex conductivity σ :

$$\sigma = \sigma_1 - j \cdot \sigma_2 \quad (1),$$

where the real and the imaginary components, σ_1 and σ_2 , translate directly into the normal-electron and Cooper-pair currents in a superconductor. The applicability of the Mattis - Bardeen theory to specific superconducting materials is discussed in [17], [18]. In integral form, the equations for σ_1 and σ_2 are [17]:

$$\frac{\sigma_1}{\sigma_n} = \frac{2}{\hbar\omega} \int_{\Delta}^{\infty} [f(\varepsilon) - f(\varepsilon + \hbar\omega)] \times \dots \frac{\varepsilon^2 + \Delta^2 + \hbar\omega\varepsilon}{\sqrt{(\varepsilon^2 - \Delta^2) \cdot [(\varepsilon + \hbar\omega)^2 - \Delta^2]}^{1/2}} d\varepsilon + \dots \frac{1}{\hbar\omega} \int_{\Delta}^{\hbar\omega - \Delta} [1 - 2f(\hbar\omega - \varepsilon)] \times \dots \frac{\hbar\omega\varepsilon - \Delta^2 - \varepsilon^2}{\sqrt{(\varepsilon^2 - \Delta^2) \cdot [(\hbar\omega - \varepsilon)^2 - \Delta^2]}^{1/2}} d\varepsilon \quad (2),$$

and

$$\frac{\sigma_2}{\sigma_n} = \frac{1}{\hbar\omega} \int_{\Delta - \hbar\omega, -\Delta}^{\Delta} [1 - 2f(\varepsilon + \hbar\omega)] \times \dots \frac{\varepsilon^2 + \Delta^2 + \hbar\omega\varepsilon}{\sqrt{(\varepsilon^2 - \Delta^2) \cdot [(\varepsilon + \hbar\omega)^2 - \Delta^2]}^{1/2}} d\varepsilon \quad (3),$$

where T is the temperature [K], σ_n is the normal conductivity of a superconductor just above the critical temperature T_C , $\Delta = \Delta(T)$ is the energy gap parameter [eV], $f(\varepsilon) = 1/(1 + \exp(\varepsilon/kT))$ is the Fermi function, $\omega = 2\pi f$ is the angular frequency, k is the Boltzmann's constant and \hbar is the reduced Planck's constant. The first integral of σ_1 represents conduction of thermally excited normal electrons, while the second integral of σ_1 introduces generation of quasiparticles by the incoming radiation. The lower limit on the integral for σ_2 becomes $-\Delta$ when the frequency exceeds the gap frequency. For a given superconducting material, the physical parameters are interrelated:

$$\lambda_o = \sqrt{\frac{\hbar}{\pi\mu_o\sigma_n\Delta}} \quad (4),$$

where μ_o is the permeability of vacuum. The specific surface impedance Z_s per square (unit area) of the superconducting film with thickness d is given by:

$$Z_s(\omega) = (j\omega\mu_o/\sigma)^{1/2} \coth((j\omega\mu_o\sigma)^{1/2}d) = R + jX \quad (5).$$

For the magnetic and electric field penetration depths, λ and δ_r respectively, we then can write the following expressions [18]:

$$\lambda = \frac{X}{\omega\mu_o} \quad (6), \quad \delta_r = \frac{R}{\omega\mu_o} \quad (7).$$

Equation (6) describes the behaviour of the magnetic field penetration depth vs. frequency and equation (7) gives dependence of the skin depth vs. frequency. References [14], [20] present approximations for the frequency dependence of the magnetic penetration depth in close-form equations.

Concluding, the dispersion in a superconducting microstrip transmission line has two different components, i.e., the modal

dispersion, as in any conventional microstrip line, and material dispersion due to the frequency dependence of the superconducting material properties.

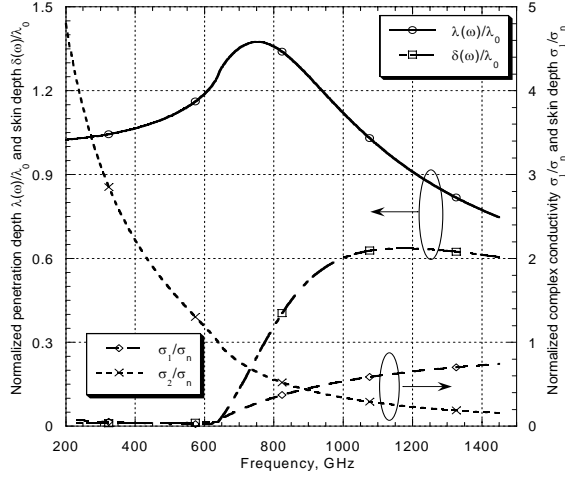


Fig. 2. Plots of the complex conductivity components, σ_1 and σ_2 , and the penetration depth of E and H components of the electromagnetic field, λ and δ , for Nb superconducting film, calculated based on Mattis-Bardeen theory. In the modeling, the Nb material parameters were as follows: $\sigma_n = 1.739 \times 10^7$ [$\Omega^{-1}\text{m}^{-1}$], $T_c = 8.1$ [K], $\lambda_0 = 8.5 \times 10^{-8}$ [m]; the calculation was made for 4 K physical temperature. At 200 GHz the magnetic field penetration depth is about 5% larger than the London penetration depth, reaching a maximum of $1.47\lambda_0$ at a frequency slightly above the gap frequency.

IV. SUPERCONDUCTING MICROSTRIP LINE MODELS WITH UNIFORM EM FIELD

Swihart [20] analyzed the SML for the case of uniform electromagnetic field with $W_{\text{ground}} \gg W \gg h$ (Fig. 1) and found a solution for the Maxwell equations in that case, with the line characteristic impedance and the propagation constant expressed as follows:

$$Z_o = \frac{120\pi}{\sqrt{\epsilon_r}} \cdot \frac{h}{W} \cdot \sqrt{1 + \frac{\lambda_o \coth(t_s/\lambda_o) + \lambda_o \coth(t_g/\lambda_o)}{h}} = Z_p \times Sw^{0.5} \quad (8)$$

$$\beta_o = \frac{2\pi}{\Lambda_o} \cdot \sqrt{\epsilon_r} \cdot \sqrt{1 + \frac{\lambda_o \coth(t_s/\lambda_o) + \lambda_o \coth(t_g/\lambda_o)}{h}} = \beta_p \times Sw^{0.5} \quad (9)$$

$$Sw = 1 + \frac{\lambda_o \coth(t_s/\lambda_o) + \lambda_o \coth(t_g/\lambda_o)}{h} \quad (9a)$$

where Λ_o is the free space wavelength, Z_p and β_p are the characteristic impedance and the wave propagation constant of the line with the same geometry, the uniform field distribution and made of a perfect conductor; the rest of the parameters in equations (8), (9) and (9a) are dimensional parameters of the superconducting microstrip line (Fig. 1). Here and through the entire paper, we assume for simplicity that the strip and ground electrodes are made from the same type of superconducting material.

Equations (8) and (9) have a very simple physical interpretation; the electromagnetic field penetrates into the

strip and ground superconducting electrodes of the microstrip transmission line at the effective depth of λ_o , the London penetration depth, extending the space where the electromagnetic wave propagates beyond the thickness of dielectric, h . Similar phenomenon occurs in a microstrip line made from a normal conductor with the thickness of the dielectric comparable with the *skin depth* in the strip and ground conductors, as presented in [22]. The Swihart solution assumes that the magnetic field penetration depth is the static London penetration depth, λ_o , independent on frequency of the electromagnetic wave propagating inside the microstrip line.

With the same assumption about the field uniformity in the SML, Kautz [17] has applied the theory of Mattis and Bardeen, taking into account that the behaviour of the superconducting material depends on the frequency. At frequencies close to the superconducting material gap frequency, the conducting properties of the superconductor are described by the anomalous skin effect with the superconductor surface impedance presented via its complex conductivity as discussed above. Kautz presented calculations of the SML impedance, the propagation constant and loss in the line for a wide frequency band.

However, both models [17], [20] neglect the fringing component of the electromagnetic field, which contributes substantially and give an error up to 30% of the line characteristic impedance and the wave propagation constant of a SML.

V. SUPERCONDUCTING MICROSTRIP LINE MODELS WITH FRINGING FIELD INCLUDED

The behaviour of a superconducting microstrip transmission line taking into account the fringing fields was analyzed by a number of authors [4]–[8]. Two approaches are used to obtain the parameters of the superconducting microstrip line. The first approach is, as for a conventional microstrip, to solve the Maxwell equations for a given geometry and boundary conditions, using, e.g., conformal mapping [7], and deriving close form equations for the SML impedance and wave propagation constant. Another approach to obtain the characteristic impedance and the wave propagation constant in SML uses the surface impedance of the superconductors comprising the line. The surface impedance, derived by employing the Mattis-Bardeen theory, is included in the calculations of the line characteristic impedance and the wave propagation constant by taking into account a geometry factor, i.e., the RF current distributions in the strip and ground electrodes, for example, in [5], [6], [8]. Interestingly, the result obtained by Swihart, who assumed an uniform field distribution, shows that the superconducting material contribution appears as a multiplier for both characteristic impedance and wave propagation constant, equation (8), (9) and (9a), compared to a perfect-metal based line. Similarly, for an SML with negligible loss and the fringing field taken into account, the factorizing takes place as well [8].

In order to introduce a new model for the SML we would like to consider the influence of a superconducting material on the characteristic impedance and the propagation constant of a superconducting transmission line via analyzing a lumped model equivalent circuit of a transmission line depicted in Fig. 3a. Let us assume a lossless microstrip transmission line using a perfect conductor with radiation and dielectric material losses being negligibly small. The line equivalent circuit parameters, L and C , take into account the geometry and the effect of the *fringing field*.

Similar circuit can be used for a SML, having the same geometry as its perfect-metal based prototype, with additional

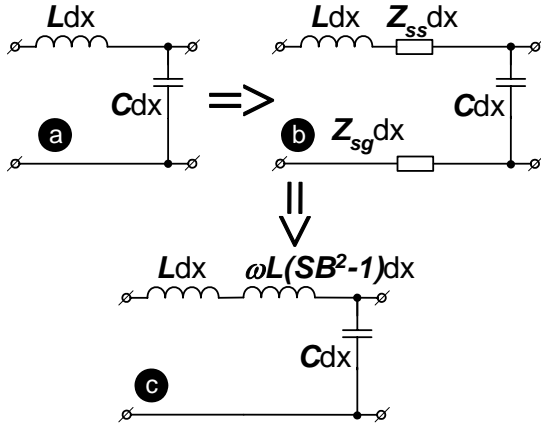


Fig. 3. Equivalent circuit of a short piece, dx , of a lossless microstrip transmission line (1) made of a perfect conductor: L is inductance and C is capacitance, per unit of length extracted using, e.g., [24]. Equivalent circuit for dx long superconducting transmission line (2 & 3): L is inductance and C is capacitance (the same as for the perfect conductor line) per unit of length. Z_{ss} and Z_{sg} are impedances of the strip and ground respectively, per unit of length describing contribution of the superconductor.

circuit components describing the superconductors, Fig. 3b. Compared to the ideal-metal-based microstrip line, the SML specific capacitance should remain unchanged since it is related to the electrostatics and therefore independent on the frequency and the current distribution inside the conductors. The specific inductance L and specific resistance R (the latter not shown in Fig. 4) are, however, subject to magnetostatics and, therefore, dependent on the RF current distribution and frequency, since the magnetic field penetration depth is frequency dependent in the superconductors. If the frequency of the electromagnetic wave propagating through the line is well below the gap frequency (about 650 GHz for Nb material used as example here) the RF conducting loss in the superconductor is negligible, $R=0$, (Fig. 3), thus the impedances Z_{ss} and Z_{sg} should be pure imaginary and *inductive*. Representing these impedances, Z_{ss} and Z_{sg} , as a product of the specific line inductance impedance, $j\omega L$, we can write the following:

$$Z_{ss}, Z_{sg} \Rightarrow j\omega L \times (SB^2 - 1) \quad (10),$$

where SB represent a correction factor for the specific inductance of the perfect conductor line and comprises both geometrical [24] and superconducting material contributions. Calculating the characteristic impedance and the wave

propagation constant of the transmission lines, one should take into account that the series impedance and shunt admittance of the transmission line, Fig. 3a, are $Z=j\omega L$ and $Y=j\omega C$ and correspondingly $Z=j\omega L+(Z_{ss}+Z_{sg})$ and $Y=j\omega C$ for SML for the equivalent circuit shown in Fig. 3b, 3c. We arrive to the following equations:

- for the perfect conductor based microstrip line, the characteristic impedance Z_p and wave propagation constant β_p are:

$$Z_p = \sqrt{\frac{\omega L}{\omega C}} = \sqrt{\frac{L}{C}} \quad \text{and} \quad \beta_p = \sqrt{\omega^2 LC} = \omega \sqrt{LC} \quad (11);$$

- for the superconducting microstrip line, the characteristic impedance Z_s , taking into account equation (10), is:

$$Z_s = \sqrt{\frac{\omega L + \omega L \times (SB^2 - 1)}{\omega C}} = SB \times \sqrt{\frac{L}{C}} = SB \times Z_p \quad (12),$$

and the wave propagation constant β_s is:

$$\beta_s = \sqrt{(\omega L + \omega L \times (SB^2 - 1)) \times \omega C} = \dots \quad (13),$$

$$\dots \sqrt{\omega^2 SB^2 \times LC} = SB \times \omega \sqrt{LC} = SB \times \beta_p$$

where L and C are the equivalent inductance and shunt capacitance of the line based on a perfect conductor.

The correction factor SB depends, in general, on the surface impedance of the strip and ground electrodes constituting the microstrip line, see equations (1–5) and on the geometrical factor of the field penetration including the RF current distribution effects.

G. Yassin and S. Withington [7] introduced a penetration factor, χ , that is a parameterized H-field penetration in the superconductors of a microstrip line and is a function of the line geometry. The calculations of χ , made in [7] for different geometries of the SML (Fig. 4), show that when the SML strip conductor is relatively thin, $t_s/h \leq 0.1$, and narrow, $W/h \leq 7$, the penetration factor χ is different from unit, indicating difference in the field penetration compare to the case of the uniform field distribution when $\chi \rightarrow 1$.

Practical considerations and thin-film technology limitations constrain the range of useful and attainable SML geometries: the normalized strip thickness would be in the range of $1.2 \leq t_s/h \leq 2.3$ and the normalized strip width is of $7.7 \leq W/h \leq 50$ if we assume the use of optical lithography, the processing limitations on the dielectric and metal layer thicknesses, etc. Summarizing, the SML line with geometries of interest has the field penetration factor $\chi \cong 1$, that is *very close* to that of the line with uniform field distribution, Fig. 4.

Based on that fact and referring the equations (8, 9), (11, 12) and (9a), we can write a new equation for the correction factor SB :

$$SB = \sqrt{1 + \frac{\lambda(\omega) \cdot \coth(\frac{t_s}{\lambda(\omega)}) + \lambda(\omega) \cdot \coth(\frac{t_g}{\lambda(\omega)})}{h}} \quad (14),$$

$$\text{and } \lambda(\omega) = \frac{X(\omega)}{\omega \mu_0}$$

In equation (14) we bear in mind the Swihart solution for the static (frequency independent) London penetration depth,

λ_0 , as in equation (9a), and use similarity of equation (8, 9) with equations (12, 13), suggesting that $SB \propto \sqrt{Sw}$, which should be exact for $W \gg h$ and *zero frequency*. Taking into account that the H-field penetration depth is a *frequency dependent quantity*, as it is clear from equation (6), and considering that $\lambda(\omega)$ is a slow function of the frequency, Fig. 2, we use the frequency dependent $\lambda(\omega)$ in the Sw factor, equation (9a), suggesting the Swihart solution to be valid for every single frequency.

Summarizing, the proposed new model takes into account the fact that contribution of the superconducting strip and ground conductors to the microstrip line performance can be represented in the form of the SB multiplier factor, equation (14). The SML characteristic impedance and the propagation factor are obtained from those of a microstrip line with the same geometry based on ideal conductors, which includes the effect of the *fringing field*, and scaled by the SB factor.

The presented model was successfully used for a number of SIS mixer projects [16], [20], [25] – [28] demonstrating its

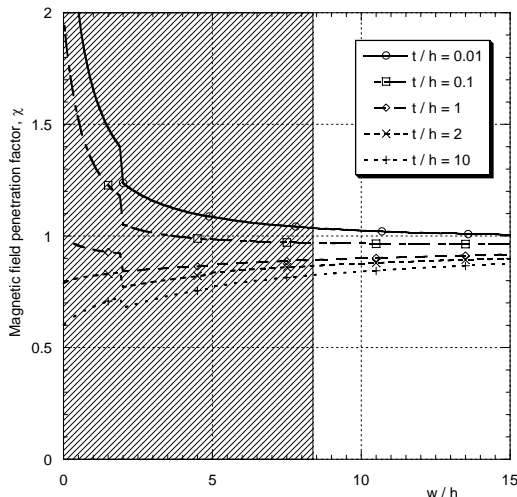


Fig. 4. The penetration factor χ is shown as a function of normalized strip width w/h for various strip thicknesses: $t/h = 10, 2.0, 1.0, 0.5, 0.1, 0.01$. The hatched area in the plot shows the region where the magnetic field penetration factor is substantially higher or lower than $\chi = 1$ and is beyond the range of attainable SML geometries.

high accuracy. However, the accuracy of the model was judged indirectly, via the achieved performances of the SIS mixers. Clearly, the precision of the new model depends on the correctness of the conventional microstrip line model, e.g., [23], employed to calculate the line characteristic impedance and effective dielectric constant. The accuracy of SB -factor describes the contribution of the superconducting material for particular SML geometry and the magnetic field penetration pattern.

VI. NUMERICAL SIMULATION OF SML WITH HFSS

The SML was simulated using 3-D electromagnetic field numerical simulation package, HFSS. We used the approach suggested by A.R. Kerr [13], where a superconductor of finite thickness T is represented by two infinitely thin conducting

sheets (Fig. 5) having a corrected surface impedance. The corrected surface impedance is calculated based on the surface impedance of the actual superconductor, equation (5), and the fact that the two surfaces interact via the penetration of the magnetic field (the thickness T is assumed to be comparable with the magnetic field penetration depth λ).

The equation for the surface impedance in the HFSS simulation was modified for term β , reference [13]; the introduced modifications reflect the fact that the magnetic field penetration is frequency dependent. Therefore, the surface impedance of the superconductor of the thickness T , having its bulk surface impedance $Z_s(\omega)$, equation (5), is as the following:

$$Z_x(\omega, T) = Z_s(\omega) \times \left[1 - \frac{j\omega\mu_0 T}{2 \cdot Z_s(\omega)} + \sqrt{1 + \left(\frac{j\omega\mu_0 T}{2 \cdot Z_s(\omega)} \right)^2} \right] \quad (15)$$

Based on equation (15), the ground plane is presented in HFSS as two conducting sheets separated by a distance t_g with the surface impedance $Z_{\text{ground}}(\omega) = Z_x(\omega, t_g)$, Fig. 1, 5. Employing the same approach, we should represent the strip as a rectangular boxed structure with conducting sheets having the surface impedance in the horizontal plane $Z_{\text{strip}_h}(\omega) = Z_x(\omega, t_s)$ and the vertical plane surface impedance $Z_{\text{strip}_v}(\omega) = Z_x(\omega, W)$, as depicted in Fig. 5.

However, considerations about the field structure at the edges of the strip lead us to the conclusion that the surface impedance of the vertical and horizontal sheets should vary continuously along the perimeter of the rectangular box that represents the superconducting strip in the HFSS simulations. Furthermore, the RF current in a microstrip line is largely concentrated around the strip edges; for the superconducting strip, the current distribution is even more prominent, [28]. This makes the results of HFSS simulation sensitive to the surface impedance of the strip edges and, in our view, should be the main accuracy limitation in the presented HFSS simulation approach.

VII. SML MODELS' COMPARISON

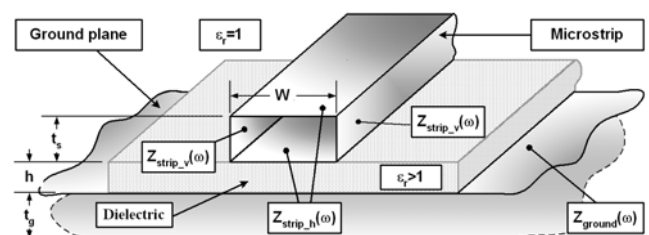


Fig. 5. Simulation of the SML in finite-element solver (HFSS). The strip is simulated as a box structure with conducting sheets having different surface impedances for vertical and horizontal planes.

In order to establish a common reference for the models' comparison we used Nb-based SML with the following material properties: the normal state conductivity, $\sigma_n = 1.619 \times 10^7 \text{ } [\Omega^{-1}\text{m}^{-1}]$, critical temperature, $T_c = 8.7 \text{ [K]}$, London penetration depth, $\lambda_0 = 8.5 \times 10^{-8} \text{ [m]}$ and ambient

temperature $T = 4.2$ K. This combination of the material parameters results in the superconducting gap $\Delta = 1.377$ mV at 4.2 K. The frequency range of interest is 80 - 1080 GHz. For our simulation we have chosen SiO_2 as the dielectric ($\epsilon_r = 3.74$) with several thicknesses of 150, 250 and 450 nm. The penetration depth, λ_o , is a superconducting material constant of an absolute value for a given material. In order to account for the magnetic field penetration we used absolute thickness of the dielectric material in the modelling, as above, and the strip width of 2, 4, 6 and 10 μm for each thickness of the dielectric, rather than usually used relative ratio of the dielectric thickness, t/h , and the strip width, w/h . This ensured that we use correct description of the SML at the condition when the strip and ground conductor and the dielectric layer thicknesses are comparable with the magnetic field penetration depth. In the modelling, the strip and the ground plane were assumed to have the same thicknesses. In order "to align" W.H. Chang model, [4], and make it more representative in the comparison with the more recent models, we introduced frequency dependence of the H-field penetration depth $\lambda = \lambda(\omega)$, equations (1 – 7), and used it *instead* of λ_o as originally proposed by W.H. Chang.

Starting point for every model was the line geometry, Fig. 1, the superconducting material parameters and, if required, the surface impedance calculated for every thickness of the Nb material. The simulation of the models from references [4], [7] and the new model introduced in this article was done using MathCAD [29]. The SML model used in Caltech [5], [6] was realized in the *SuperMIX* software package [30] and the original code was used to model the described above SML geometries. We have chosen to plot the characteristic impedance and a slow-wave factor or the wavelength ratio, $\Lambda_{\text{free_space}}/\Lambda_{\text{in_line}}$, in order to characterize the electromagnetic wave propagation in the SML for different models (see Fig. 6 – 17 below)

VIII. DISCUSSION

The results of the simulations show a trend for both the SML impedance and the slow-wave factor to follow the dependence of the penetration depth vs. frequency. The spread in the modelling results is slightly larger in the slow-wave factor while the results on the characteristic impedance calculations show more consistency. As expected, introducing the frequency dependent H-field penetration produces drastic changes in the SML impedance and the slow-wave factor, $\Lambda_{\text{free_space}}/\Lambda_{\text{in_line}}$, those become up to 30% higher for thin dielectric (150 nm) around the gap frequency compared to, e.g., at 100 GHz.

The new model produces results, which are the most close to the HFSS simulations and the model presented by G. Yassin & S. Withington (YW-model) for all investigated SML geometries. Maximum discrepancy between the new model, as compared to YW-model and HFSS simulation, is of about 5% and occurs for 2 μm wide strip between 600 and 800 GHz. For the rest of 80-1080 GHz band the error not

exceed 2.5 % for all geometries. The SiO_2 dielectric thickness of 650nm was modelled as well showing consistent results but not included here due to being less interesting for practical applications.

HFSS simulations and YW-model results differ up to 4.5% without clear frequency dependence pattern. Surprisingly, the biggest discrepancy occurs for the widest strip width, 10 μm , and the thinnest dielectric, 150 nm. Presence of such a difference between YW-model on one side and HFSS on another brings us to the conclusion that perhaps further refinements should be made in HFSS approach to use more realistic distribution of the surface impedance of the strip edges. The discrepancy leaves open the question about the reference model.

The new model, presented in this paper, requires relatively simple calculation procedures, especially compared to HFSS simulation; the computation could be further simplified if one of the approximation functions for $\lambda(\omega)$ is used [14], [20]. Interestingly, the new model that initially does not take into account the loss in the superconductors and its increasing at frequencies above the gap frequency, anyways, produces *correct* values for the real part of the line impedance and the slow-wave factor as compared to HFSS simulations and YW-model, with the latter taking use of the superconductor surface impedance and therefore including these losses. This opens the possibility to use the suggested model even in the *wider* frequency band by adding conventional multiplicative loss factor [32].

ACKNOWLEDGMENT

Authors would like to thank Prof. R.S. Booth for his remarkable support through the course of our work. We are thankful to Dr. A.R. Kerr for useful discussions about numerical simulations of superconductors using HFSS and colleagues from Caltech for generous sharing of the *SuperMIX* software. We greatly appreciate Mathias Fredrixon for his continuous effort to keep our computing facilities in a good shape.

Authors would like to thank *Dr. R. Laing* and *Dr. D. Emerson*, who made it possible to publish this article as ALMA Memo.

A shorten version of this paper was published in the Int. Journal of Infrared and Millimeter Waves, Vol.27, No. 6, pp. 809-834, June 2006, ISSN 0105-9271, Springer, V. Belitsky, C. Risacher, M. Pantaleev, V. Vassilev, "Model Study of Superconducting Microstrip Line at Millimeter and Sub-Millimeter Waves".

REFERENCES

- [1] J.R. Tucker, M.J. Feldman, "Quantum detection at millimeter wavelengths", *Rev. Modern Phys.*, vol. 4, pp. 1055-1113, 1985.
- [2] M. J. Wengler, "Submillimeter-Wave Detection with Superconducting Tunnel Diodes," *IEEE Proc.*, vol. 80, pp. 1810-1826, 1992.
- [3] R. Blundell and C.-Y. Tong, "Submillimeter Receivers for Radio Astronomy," *IEEE Proc.*, vol. 80, pp. 1702-1720, 1992.
- [4] W.H. Chang, "The inductance of a superconducting strip transmission line", *J. Appl. Phys.*, vol. 50, no. 12, pp. 8129 - 8134, Dec. 1979.
- [5] J. Zmuidzinas, H.G. LeDuc, "Quasi-Optical Slot Antenna SIS Mixers", *IEEE Trans. Microwave Theory Tech.*, vol. 40, pp. 1797-1804, 1992.
- [6] M. Bin, "Low Noise THz Niobium SIS Mixers", Ph.D. dissertation, Cal. Inst. of Tech, October 1997.
- [7] G. Yassin and S. Withington, "Electromagnetic models for superconducting millimetre-wave and sub-millimetre-wave microstrip transmission lines", *J. Phys. D: Appl. Phys.*, vol. 28, pp. 1983-1991, 1995.
- [8] C.-Y. Tong, R. Blundell, S. Pain, D.C. Papa, J. Kawamura, X. Zhang, J.A. Stern, H.G. LeDuc, "Design and Characterization of a 250-350 GHz Fixed-Tuned Superconductor-Insulator-Superconductor Receiver", *IEEE Trans. Microwave Theory and Tech.*, vol. 44, Iss. 9, pp. 1548 - 1556, 1996.
- [9] J. Bardeen, L.N. Cooper, J.R. Schrieffer, "Theory of Superconductivity", *Phys. Rev.*, 1957.
- [10] T. Imamura, T. Shiota and S. Hasuo, "Fabrication of High Quality Nb/AIOx-Al/Nb Josephson Junctions: I - Sputtered Nb films for junction electrodes.", *IEEE Trans. on Appl. Superconductivity*, vol. 2, no. 1, pp. 1-14, 1992.
- [11] T. Imamura, S. Hasuo, "Fabrication of High Quality Nb/AIOx-Al/Nb Josephson Junctions: II - Deposition of Thin Al Layers on Nb Films", *IEEE Trans. on Appl. Superconductivity*, vol. 2, no. 2, pp. 84-94, 1992.
- [12] Agilent High-Frequency Structure Simulator (HFSS), Agilent Technologies, 395 Page Mill Road, Palo Alto, CA 94304, U.S.A.
- [13] A.R. Kerr, "Surface Impedance of Superconductors and Normal Conductors in EM Simulators", *Electronics Division Internal Report No. 302*, NRAO, February 1996.
- [14] G.S. Lee and A. T. Barfknecht, "Geometrical and Material Dispersion in Josephson Transmission Lines," *IEEE Trans. on Appl. Superconductivity*, vol. 2, pp. 67-72, 1992.
- [15] H.H.S. Javadi, W. R. McGrath, B. Bumble, and H. G. LeDuc, "Onset of Dispersion in Nb Microstrip Transmission Lines," *Proceedings of the III Int. Symp. on Space Terahertz Technology*, Univ. of Michigan, Ann Arbor, USA, 1992, pp. 362 - 381.
- [16] V. Belitsky, S. W. Jacobsson, L.V. Filippenko, E.L. Kollberg, "Theoretical and Experimental Studies of Nb-based Tuning Circuits for THz SIS Mixers", *Proceedings of the 6th Space Terahertz Technology Symposium*, Caltech, Pasadena, USA, March 21-23, 1995, pp. 87 - 102.
- [17] R.L. Kautz, "Picosecond pulses on superconducting striplines," *J. Appl. Phys.*, vol. 49, pp. 308 - 314, 1978.
- [18] R. Pöpel, "Surface impedance and reflectivity of superconductors," *J. Appl. Phys.*, vol. 66, pp. 5950 - 5957, 1989.
- [19] D.C. Mattis and J. Bardeen, "Theory of anomalous skin effect in normal and superconducting metals", *Phys. Rev.*, vol. 111, pp. 412 - 417, 1958.
- [20] V. Belitsky, S.W. Jacobsson, L.V. Filippenko, C. Holmstedt, V.P. Koshelets, E.L. Kollberg, "Fourier Transform Spectrometer Studies (300-1000 GHz) of Nb-based Quasi-Optical SIS Detectors", *IEEE Trans. on Appl. Supercond.*, vol. 5, Nov. 3, pp. 3445 - 3451, 1995.
- [21] J.C. Swihart, "Field Solution for a Thin-Film Superconducting Strip Transmission Line", *J. Appl. Phys.*, vol. 32, no. 3, 1961, pp.461-469.
- [22] F. Schnieder, W. Heinrich, "Model of Thin-Film Microstrip Line for Circuit Design", *IEEE Trans on MTT*, vol. 49, no. 1, pp. 104 - 110, 2001.
- [23] E.O. Hammerstad and Ø. Jensen, "Accurate Models for Microstrip Computer Aided Design", *IEEE MTT-S International Microwave Symposium Digest*, pp.407 - 409, 1980.
- [24] R.A. Pucel, D.J. Massé and C.P. Hartwig, "Losses in microstrip", *IEEE Trans. Microwave Theory Tech.*, vol. 16, 1968, pp. 342-350; see also correction in vol. 16, 1968, p. 1064.
- [25] S.W. Jacobsson, V. Belitsky, L.V. Filippenko, S.A. Kovtonjuk, V.P. Koshelets, E.L. Kollberg, "Quasi-optical 0.5 THz SIS Receiver with Twin Junctions Tuning Circuit", *The 18th Int. Conf. on Infrared and Millimetre Waves*, Univ. of Essex, UK, vol. SPIE 2104, 1993, pp. 267-268.
- [26] V. Belitsky, I.L. Serpuchenko, M.A. Tarasov, A.N. Vystavkin, "MM Waves Detection Using Integrated Structure with SIS Junction, Stripline Transformer and Spiral Antenna", *Extended Abstracts of ISEC'89*, Tokyo, Japan, 1989, pp. 179-182.
- [27] V. Belitsky, M.A. Tarasov, S.A. Kovtonjuk, L.V. Filippenko, O.V. Kaplunenko, "Low Noise Completely Quasioptical SIS Receiver for Radioastronomy at 115 GHz", *Int. J. Infrared and Millimetre Waves*, vol. 13, no. 4, pp. 389-395, 1992.
- [28] V. Vassilev, V. Belitsky, C. Risacher, I. Lapkin, A. Pavolotsky, E. Sundin, "A Sideband Separating Mixer for 85-115 GHz", Accepted for publication in *IEEE Microwave and Wireless Components Letters*, November 2003.
- [29] D.M. Sheen, S.M. Ali, D.E. Oates, R.S. Withers, J.A. Kong, "Current Distribution; Resistance, and Inductance for Superconducting Strip Transmission Lines", *IEEE Trans. on AP*, vol. 1, no. 2, pp. 108 - 115, 1991.
- [30] MathCAD 2000i, Mathsoft Corp., <http://www.mathsoft.com>.
- [31] SuperMix, <http://www.submm.caltech.edu/supermix/default.html>.
- [32] S.R. Pennock, P.R. Shepherd, "Microwave Engineering with Wireless Applications", Macmillan Press, ISBN 0-333-72801-7, 1998.

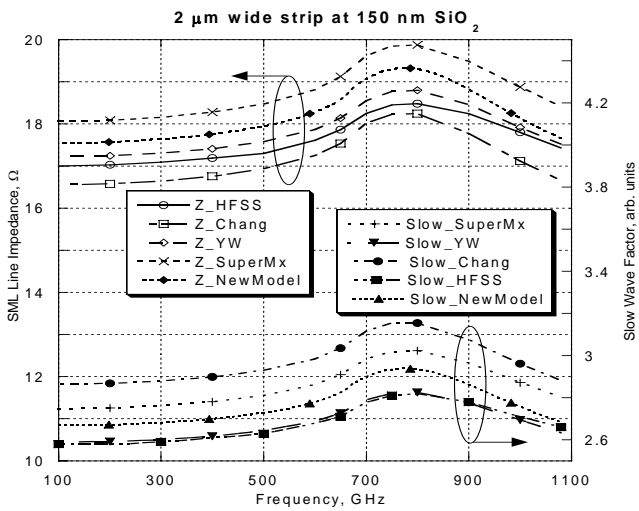


Fig. 6. Simulation results of the SML with 2 μm wide strip and 150 nm thick SiO_2 dielectric.

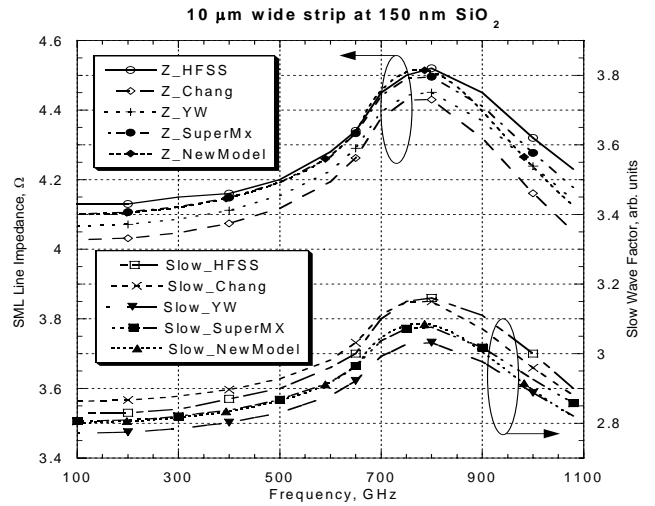


Fig. 9. Simulation results of the SML with 10 μm wide strip and 150 nm thick SiO_2 dielectric.

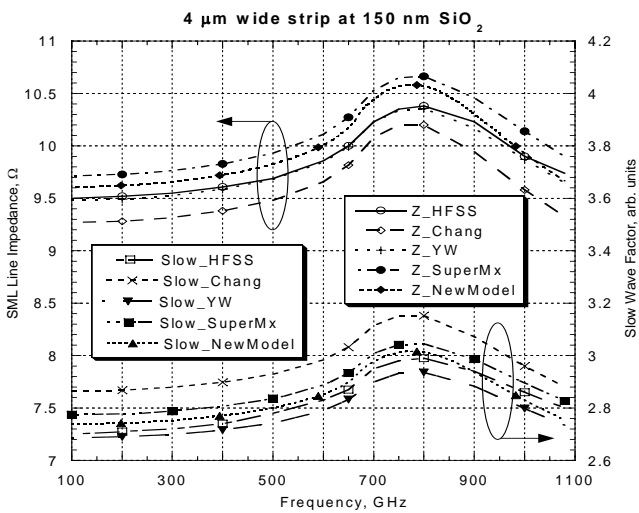


Fig. 7. Simulation results of the SML with 4 μm wide strip and 150 nm thick SiO_2 dielectric.

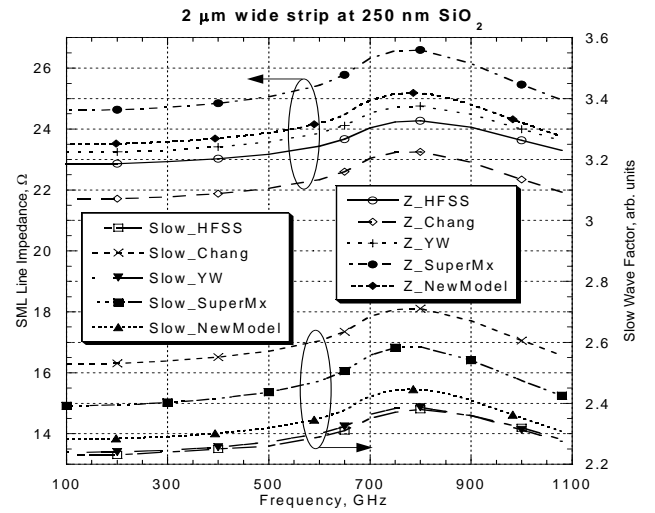


Fig. 10. Simulation results of the SML with 2 μm wide strip and 250 nm thick SiO_2 dielectric.

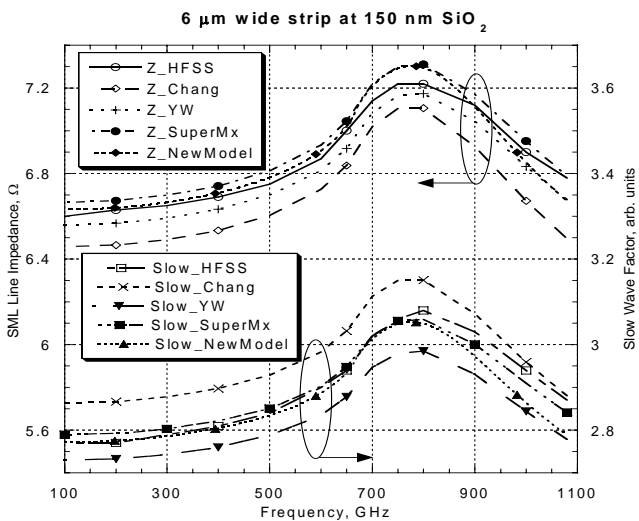


Fig. 8. Simulation results of the SML with 6 μm wide strip and 150 nm thick SiO_2 dielectric.

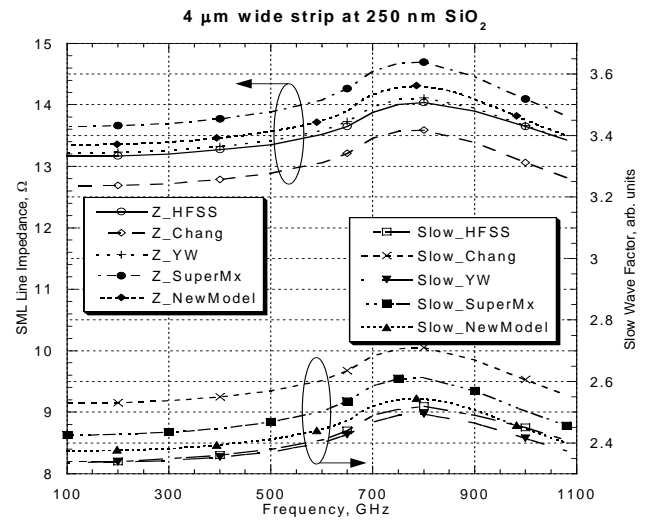


Fig. 11. Simulation results of the SML with 4 μm wide strip and 250 nm thick SiO_2 dielectric.

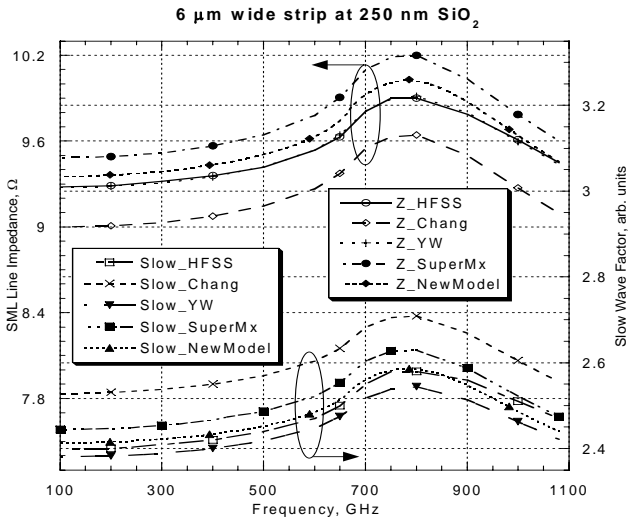


Fig. 12. Simulation results of the SML with 6 μm wide strip and 250 nm thick SiO_2 dielectric.

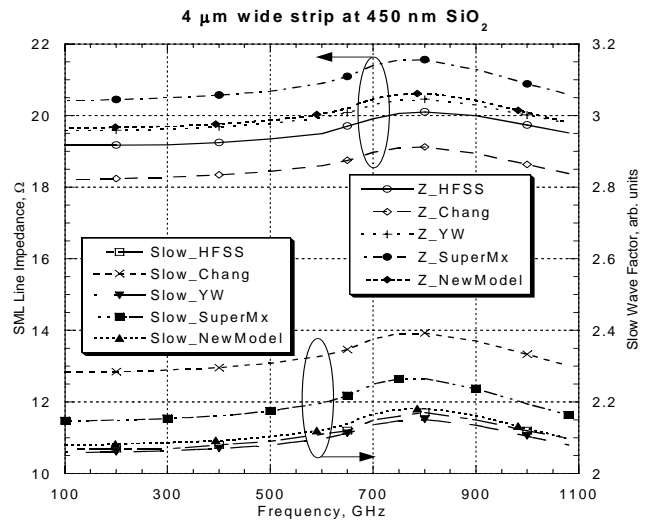


Fig. 15. Simulation results of the SML with 4 μm wide strip and 450 nm thick SiO_2 dielectric.

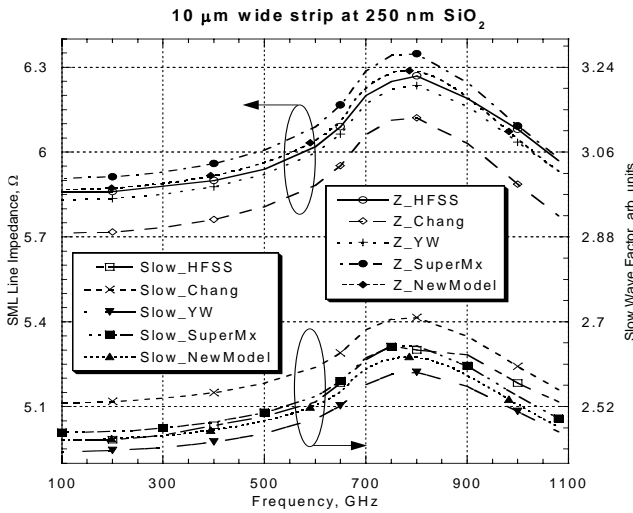


Fig. 13. Simulation results of the SML with 10 μm wide strip and 250 nm thick SiO_2 dielectric.

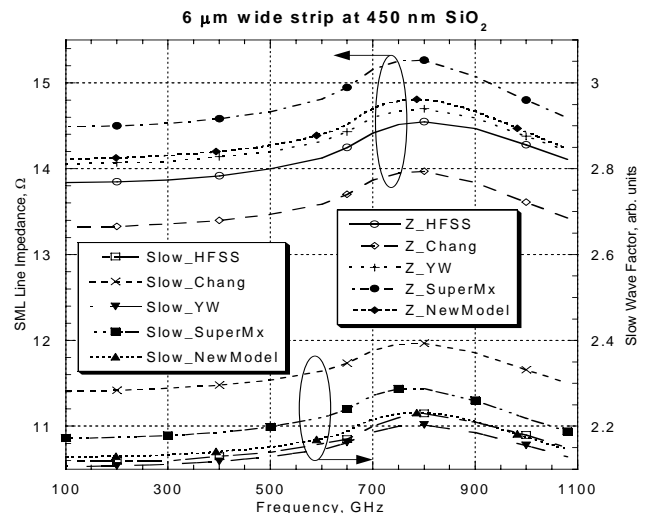


Fig. 16. Simulation results of the SML with 6 μm wide strip and 450 nm thick SiO_2 dielectric.

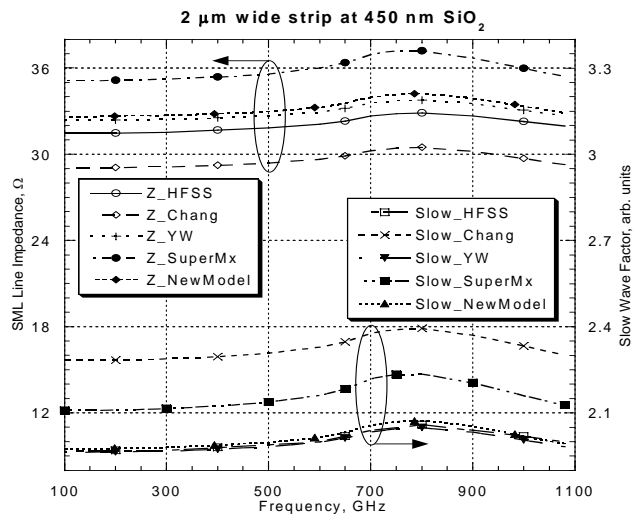


Fig. 14. Simulation results of the SML with 2 μm wide strip and 450 nm thick SiO_2 dielectric.

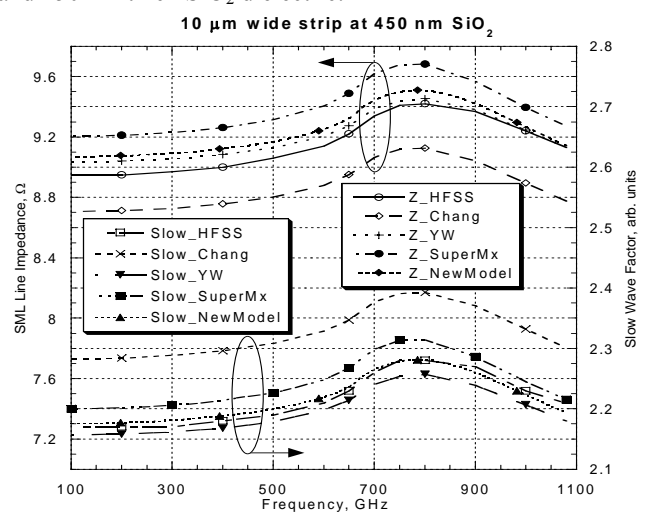


Fig. 17. Simulation results of the SML with 10 μm wide strip and 450 nm thick SiO_2 dielectric.